WADC-TN-59-93
AD 212564

STUDY OF LIQUID GAS INTERFACE DURING DISCHARGE FROM THE B-1A FIRE-EXTINGUISHING AGENT CONTAINER

Ralph L. Hough

Aeronautical Accessories Laboratory

APRIL 1959

Project No. 6075

WRIGHT AIR DEVELOPMENT CENTER

WADC-TN-59-93
AD 212564

STUDY OF LIQUID GAS INTERFACE DURING DISCHARGE FROM THE B-1A FIRE-EXTINGUISHING AGENT CONTAINER

Ralph L. Hough

Aeronautical Accessories Laboratory

APRIL 1959

Project No. 6075

WRIGHT AIR DEVELOPMENT CENTER

100 — September 1959 — 3-108

TABLE OF CONTENTS

LIST OF ILLUSTRATIONS

LIST OF TABLES

I. INTRODUCTION

Integral to an airborne fire extinguishing system is the extinguishing agent storage facility. Frequently the storage facility is in the form of a sphere with suitable charging, overheat, and agent discharge fixtures. The spherical form has the obvious advantage over other forms in that a smaller quantity of wall material can be made to contain a given volume.

Most of the extinguishing agents used in the sphere are in the liquid phase during storage. Many exhibit little change in phase during the discharge process. The agent is expelled by a charge of nitrogen gas, perhaps supplemented by the vapor pressure of the agent. Commonly used by the Air Force is bromochloromethane (CB), a liquid at room temperature. This agent is expelled by a charge of nitrogen gas stored in the sphere at a pressure of 400 to 440 psig at 70°F. Normally the bromochloromethane occupies 50 percent of the internal volume of the sphere. Other agents include dibromodifluoromethane (DB), bromotrifluoromethane (BT) and carbon dioxide (CO_2).

The possible lack of conformation of the gas-liquid interface to a flat plane during the discharge process has been a subject of debate. In what manner, if any, and to what degree is this interface distorted? If the interface distorts to any great extent, propellant gas will tend to bypass considerable portions of agent. This bypass effect will then give rise to a discontinuous flow of agent from the container during the latter portion of the discharge process. Some of the stored energy of the expanding propellant gas will not be transferred to the entire agent mass. The efficient use of that portion of agent bypassed will then be materially reduced.

If propellant bypass poses a serious problem, one solution would be to choose an agent with sufficiently high vapor pressure so that only the gaseous state would exist in the container. Stated otherwise, eliminate the bypass problem by eliminating the gas-liquid interface. This solution is inadvisable, however, in that the container walls would have to be thick enough to resist the increased storage pressures involved. The penalty of increased container weight would probably more than cancel any gain obtained through elimination of the interface.

Manuscript released by the author April 1959 for publication as a WADC Technical Note.

A more advisable solution would be the redesign of the container to eliminate propellant bypass. Although the use of a sphere results in a substantial savings in weight over that of another form such as a cylinder, for example, other factors may offset this advantage. The difficult and sometimes complex mounting requirements of a sphere as compared to those of a cylinder may reduce this savings from the standpoint of both weight and fabrication complexity. Further, if a cylinder is capable of reducing the bypass phenomenon, a smaller quantity of agent contained therein might equal the fire--extinguishing capabilities of a larger quantity contained in a sphere. The net result might actually be a savings in total weight through the use of a cylinder instead of a sphere. This would depend on the manner and degree of possible distortion in the gas-liquid interface.

The material in this report, however, deals with the interface problem of the sphere only, and is based on empirical determinations. The location of fixtures in the container walls and their protrusion into the liquid mass are also briefly examined.

II. EXPERIMENTAL PROCEDURE

A. Method of Data Collection

Preliminary examination of the problem presented in collecting data indicated that direct observation of the gas-liquid interface during the discharge process would offer the best resolution. Since a transient process occurring in a total time interval of but a few seconds is best observed by high speed photography, a suitable apparatus capable of handling pressures of 400 to 600 psig was required. The apparatus devised required the internal form of a sphere and necessitated proper window material for illuminating and for photographing the interface.

B. Test Apparatus

1. Consideration of Size

Containers currently used by the Air Force are covered by MIL-C-6386 and are designated as Type B-1A. Four different sizes exist ranging in internal volume from 224 cu. in. to 945 cu. in. All sizes have the same diameter outlet port. The largest-size container (radius = approximately 6 inches) represents the extreme case of initial interface area versus outlet port area. This container should therefore exhibit the most pronounced interface distortion and should be selected as the basis for construction of the test

apparatus. The relation of interface distortion as a function of the ratio of the radii of the sphere and the outlet port is not discussed here. Rather this report deals with the experimental establishment of the existence of the distortion and the discussion of the responsible mechanism. An explanation to justify the above selection is contained in section III C.

2. Design and Construction

The largest of the B-1A type containers was selected as the basic apparatus. Preliminary discussion with photographic technicians indicated that two windows were necessary for proper cross-lighting and a third for the camera. (See Figure 1). With the wide angle lens systems available, a large portion of the interface could then be photographed. Windows 4 inches in diameter seemed best suited for the lens system. For illumination purposes the photographic technicians requested a light-reflecting surface such as cadmium plate on the interior of the sphere.

Three window mounts were designed and fabricated from 1 5/16 inch steel plate. The mounts were designed as rings 6 1/2 inches in diameter. Each mount was machined so that when welded into the upper hemisphere of the container, the internal surface of the ring retained the spherical contour of the container. A window opening 4 inches in diameter was provided. A recess half an inch deep and 5 inches in diameter was provided on the outer surface of each ring. This permitted the insertion of a gasket and a plate glass window 5 inches in diameter and 3/4 of an inch thick. A second gasket and a retaining ring held each window securely in its mounting. The retaining rings were constructed of 3/4 inch steel plate with an opening 4 inches in diameter and with a total diameter of 6 1/2 inches. Each ring was held against its respective window by twelve 1/4 inch bolts. Each glass window was

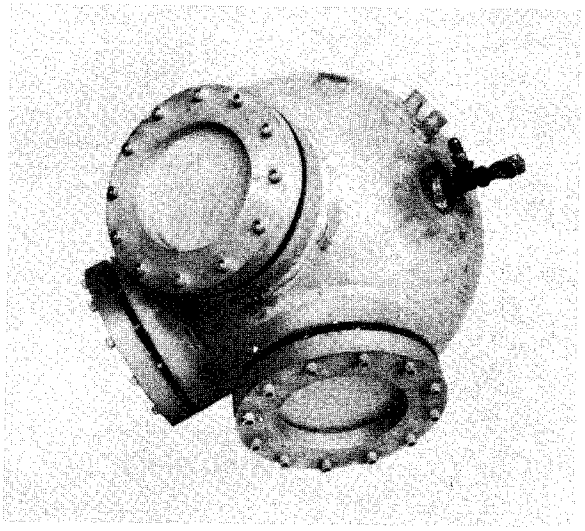

held in place such that the center of the inward face was tangent to the spherical contour of the inside of the container.

Initially the gasket material was fabricated from 1/16 inch teflon to resist the action of the estinguishing agent vapors. The windows were then mounted and the retaining rings tightened down while observing the strain pattern in the glass with the aid of a polariscope. Although no undue strain pattern was apparent at the time of mounting, a subsequent pressure test indicated the presence of strain. The container was placed in a closed cement block room equipped with a bullet-proof window and pressurized to 400 psig. At that pressure one of the windows blew out. The room was showered with particles of glass which embedded themselves in the bullet-proof window, the cement blocks and even in solid steel plates.

The surfaces of the window mountings were re-examined for irregularities and remilled when necessary. Soft silicone rubber gaskets one-eighth of an inch thick were substituted for the hard teflon gaskets. Subsequent pressure tests at 400 psig resulted in no further mishaps.

The test apparatus and camera were mounted on a framework of steel. A special shield of plywood and plexiglass was provided for the camera and lens as protection against an explosion of the window. (See Figures 2 and 3)

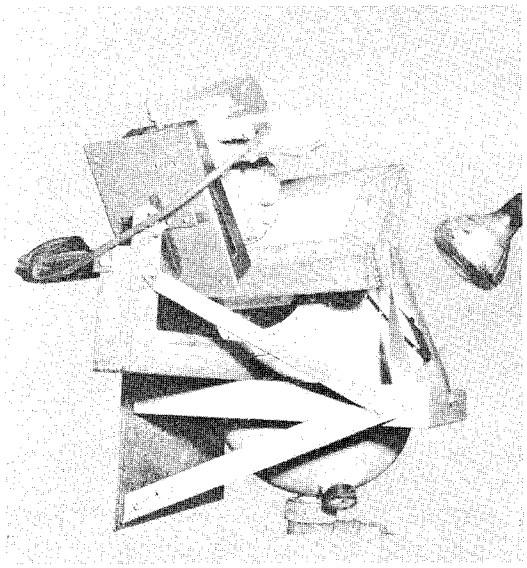

A 1/4 inch copper tube led from the apparatus to a charging setup in an adjacent room. The agent charge, if a gas at ambient pressure, could be admitted through this line. For liquid agents, a charging tank was provided near the apparatus. This tank could be filled with the liquid, pressurized to 30 or 40 psig with nitrogen and the liquid then admitted to the apparatus. The quantity of liquid charge could be adjusted by filling the tank with a measured amount of liquid or by visual observation through one of the windows. In the case of a gaseous agent, the charge could be

determined by weighing the cylinder from which the agent was drawn. The pressure could then be adjusted to the desired level with nitrogen and the copper line sealed off near the test apparatus by actuation of a solenoid valve.

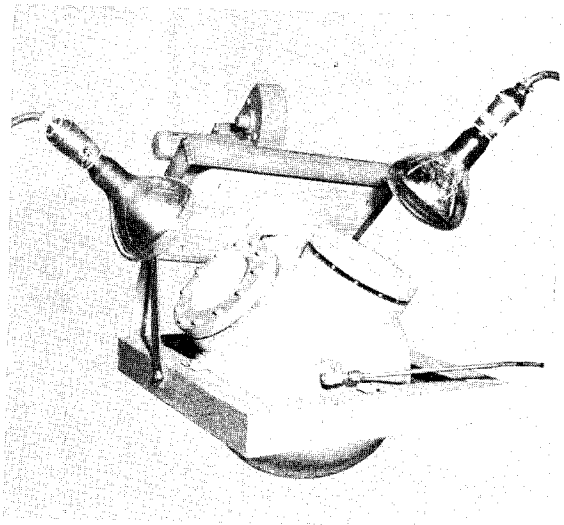

C. Conduction of Tests

A total of 15 photographic tests were conducted. (See Table I). During the course of the tests several difficulties were encountered, two of which are cited in particular.

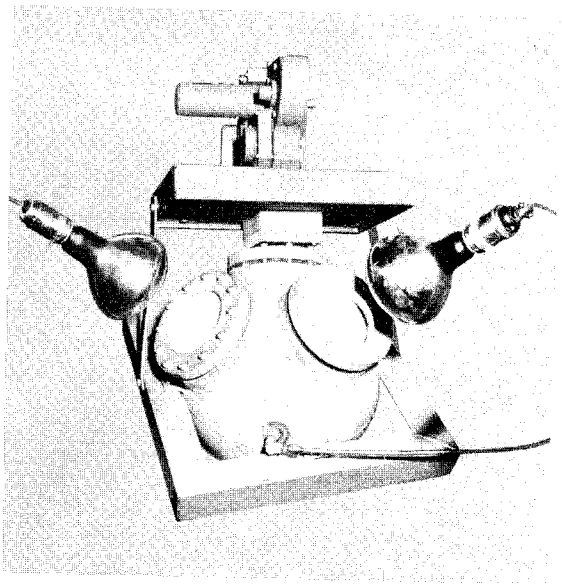

One problem developed as a result of variations in exposure time caused by the time interval in bringing the high-speed camera motor up to maximum rpm. Thus, as the discharge process progressed underexposure problems tended to increase. This difficulty was eventually reduced by using an average camera speed of one thousand frames per second at an aperture opening of f2.8.

Another problem consisted of the fogging-out of all detail on the interface shortly after initiation of the discharge. Since direct observation of the discharge process involved considerable risk, the cause of this condition was not immediately apparent. It was first believed to be due to the formation of agent vapor clouds above the liquid surface resulting from the cooling of the expanding propellant. Since the interior of the container was cadmium-plated, the reflection of light from the plating would blend with the reflection from the vapor and obscure all detail. A high boiling-point liquid, triethyleneglycol, was therefore substituted for the agents tested and colored with a red dye material containing traces of phosphor. At initial charging pressures of 100 and 200 psig good resolution of the interface pattern was obtained. At higher pressures the fogging began to recur. This indicated that the effervescent effect of dissolved nitrogen in the liquid upon release of

pressure might be the responsible mechanism. The addition of a water miscible silicone antifoamant permitted better resolution of interface detail at initial pressures of 300 and 400 psig. Thus, the change in light-reflecting properties of the interface resulting from the formation of gas bubbles appeared to be the primary cause of failure to obtain detail in the majority of the tests, with the formation of vapor clouds playing only a minor role. Sufficient resolution was obtained in Tests 9, 10, 14, and 15 to permit a general analysis of the interface change with respect to time for the liquid, triethyleneglycol.

TABLE I

TABULATION OF TESTS

Test Nr.	Agent	% Fill (By Vol.)	Pressure (psig)	Film Speed (fps)	Lens Setting	Filter	Date
1	CB[1]	50	265	1000	f5.6	Polaroid	7 Aug 58
2	CB	50	250	2000	f2.0	Polaroid	18 Aug 58
3	CB	50	250	2000	f2.0	Polaroid	19 Aug 58
4	BT[2]	18.5	240	2000	f2.0	Polaroid	19 Aug 58
5	BT	18.5	240	2000	f3.5	3N5	22 Aug 58
6	TEG[3]	50	250	2000	f3.5	3N5	22 Aug 58
7	TEG	50	250	2000	f1.5	3N5	26 Aug 58
8	TEG (red dye)	50	200	2000	f2.8		29 Aug 58
9	TEG (red dye)	50	100	1000	f2.8		3 Sep 58
10	TEG (red dye)	50	200	1000	f2.8		3 Sep 58
11	TEG (red dye)	50	300	1000	f2.8		3 Sep 58
12	TEG (red dye)	50	400	1000	f2.8		3 Sep 58
13	Water (green dye)	50	100	1000	f2.8		4 Sep 58
14	TEG[4]	50	300	1000	f2.8		9 Sep 58
15	TEG[4]	50	400	1000	f2.8		9 Sep 58

1 CB = Bromochloromethane
2 BT = Bromotrifluoromethane
3 TEG = Triethylene Glycol
4 Black dye and antifoaming agent added

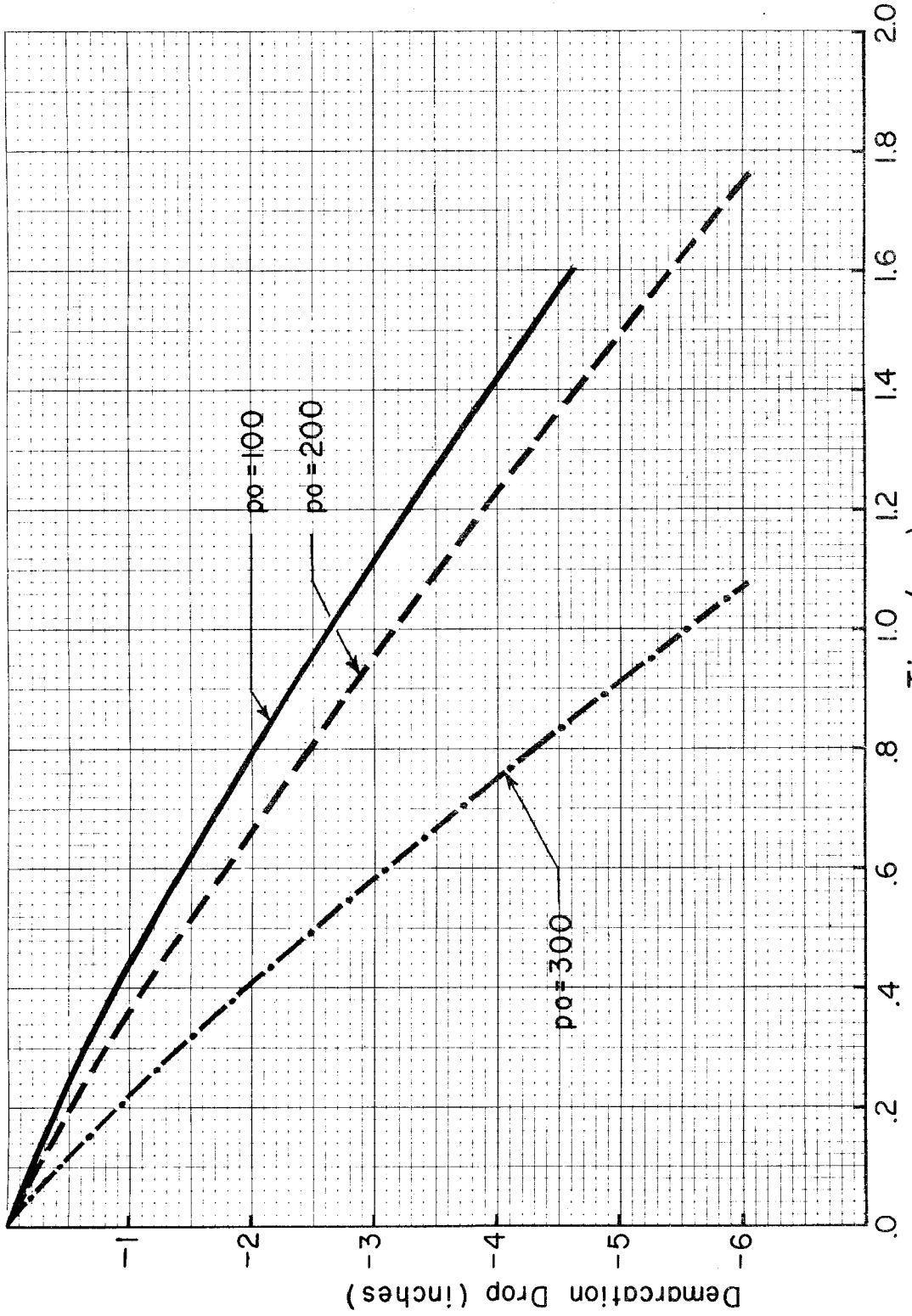

Fig 5 Observed Demarcation Drop With Respect To Time

III. INTERPRETATION OF DATA

A. Data Reduction

It is possible to determine the position of the gas-liquid interface at any given moment during the discharge process by examination of the photographic record. The problem reduces to a simple mathematical analysis of the relative positions of the interface at any given time during discharge, the initial interface, and the center of outlet port when viewed at discharge termination. The method of analysis as well as a tabulation of reduced data may be found in Appendix B. Figure 5 interprets this reduced data graphically, and indicates the position of the demarcation with respect to time for initial charging pressures, po, of 100, 200 and 300 psig.

A tabulation of container pressure during discharge may be found in Appendix C. This tabulation is for initial charging pressures of 100, 200 and 300 psig and is presented graphically in Figure 6. Figures 7, 8, and 9 represent remaining liquid volume relative to time for initial charging pressures of 100, 200, and 300 psig respectively. The graphs are presented as $Va=f(t)$ and $Vp=f(t)$, where Va is the volume of remaining liquid at time, t, as computed from the demarcation drop and Vp is the volume of remaining liquid at time, t, as computed from pressure data. (See Appendix C). Va is computed on the assumption that the interface remains planer. Vp is computed on the assumption that no propellant bypass occurs. Theoretically Va must be equal to or greater than Vp at any given moment after discharge. Figure 9 indicates a deviation from this statement. An obvious possibility is the supplying of additional N_2 by effervescence from the triethylene glycol. However, solubility tests for N_2 in

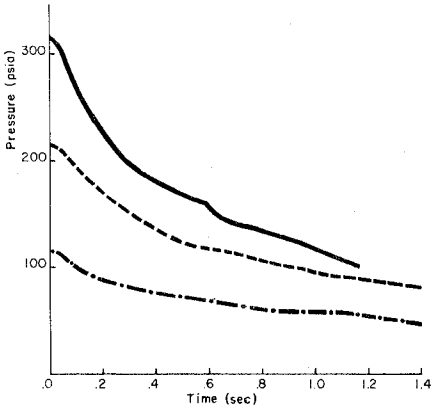

Fig 6 Container Press vs. Time

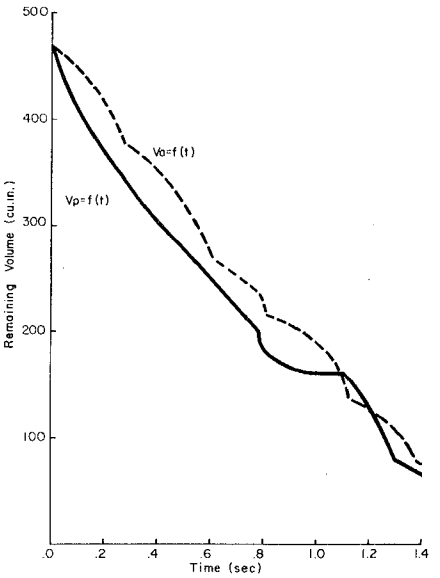

Fig 7 Vol. Decrease vs. Time at Initial Pressure of 100 psig

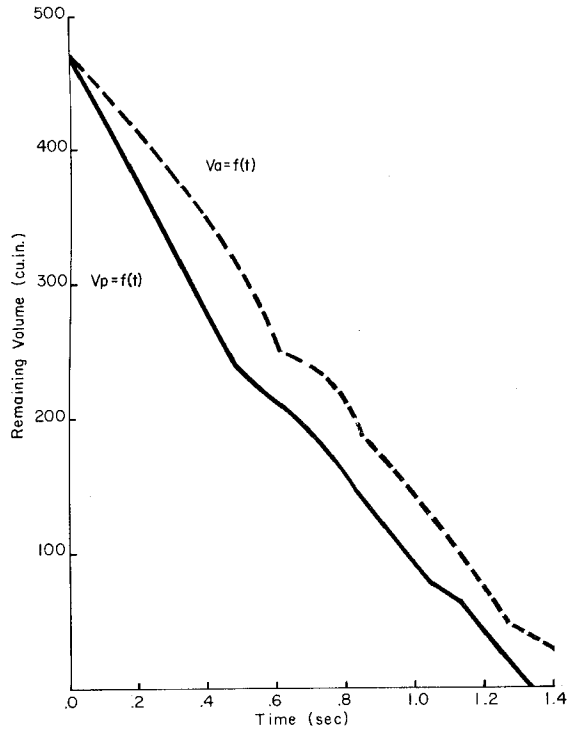

Fig 8 Vol. Decrease Vs. Time At Initial Pressure of 200 psig

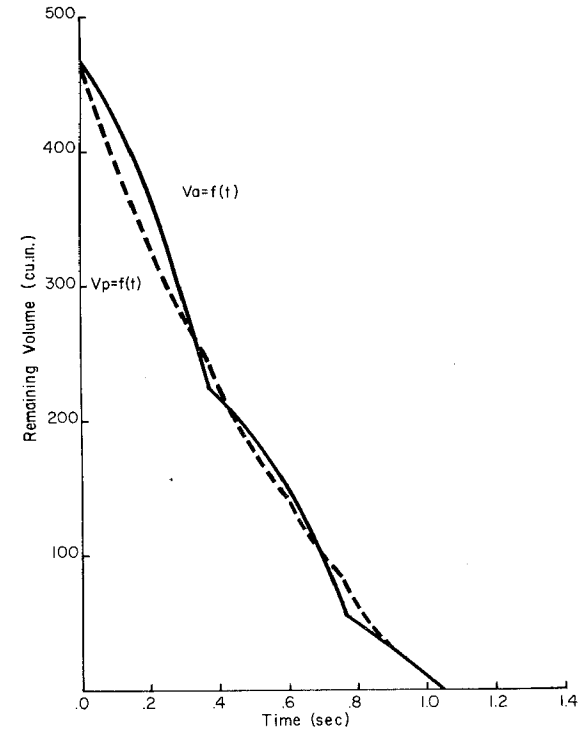

Fig 9 Vol. Decrease vs. Time At Initial Pressure of 300 psig

triethylene glycol seemingly indicated that release of dissolved N_2 from the liquid during discharge did not adversely affect the calculations. This anomaly is not given further consideration, however, and data for pressures at 300 psig was not further analyzed.

B. Analysis of Data

The analysis of the obtained data is presented in two forms, Cases I and II.

Case I deals with the consideration of a non-vorticular flow pattern and is based on the following assumptions:

(1) All fluid flow is confined to vectors normal to the outlet plane in the immediate region thereof.

(2) The discharge is, in effect, the equivalent of the expulsion of a cylindrically-shaped slug of liquid immediately above the outlet, the resultant void of which is replenished by surface flow from the interface.

(3) The interface behavior is that of a thin elastomeric membrane uniformally restrained at the perimeter and distorted by a centralized load.

Case II deals with the consideration of the interface pattern as a vorticular flow and is discussed in Section III B 2.

1. Case I

Consider Fig 10. From assumption 3 it is necessary to write the general interface contour as the surface generated by

the rotation of

(1) $y=h+F\ln\frac{a+c}{x}$

about the line x-c=o. The volume of rotation is equivalent to the calculated difference in remaining volume, Vl, as presented in Figures 7-9. For a specific time this volume becomes:

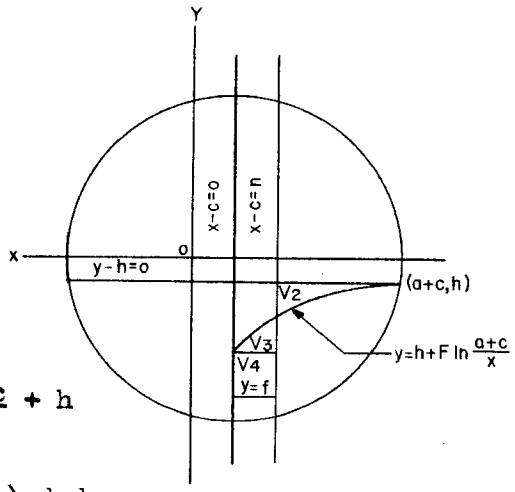

$$2\pi\int_{c}^{a+c}\int_{h}^{F\ln\frac{a+c}{x}+h}(x-c)\,dydx$$

Fig 10 Case I Model

Evaluation of the double integral yields,

(2) $V_1=\pi F(c^2\ln\frac{a+c}{c}-ac+\frac{a^2}{2})$

From assumption 2 it is evident that $V_1=\pi r^2(f-h)$, where r is the effective radius of discharge. Therefore: $V_2=V_3+V_4$

Writing the above relationship in integral form and substituting values of V_1, h, F, a and c for f we obtain:

$$\int_{r+c}^{a+c}\int_{h}^{F\ln\frac{a+c}{x}}(x-c)\,dydx=\frac{V_1}{2\pi}-\frac{r^2F}{2}\ln\frac{a+c}{c}+\int_{c}^{r+c}\int_{F\ln\frac{a+c}{x}+h}^{F\ln\frac{a+c}{c}+h}(x-c)\,dydx$$

Solving for c gives:

(3) $(c^2-r^2)\ln(a+c)=\ln c$,
or $c=r$

Substituting emperical values of V_1 and a in equation 2 together with the value c from 3, F may be computed. Equation 1 may then be evaluated in terms of x versus y. The values a and h correspond to the abscissa and ordinate respectively of the point E as given in Appendix A.

TABLE II

VARIABLE VALUES-CASE I

Pressure-100 psig

t	a	h	V_1	F(r = .308)	b(r = .308)
0	6.07	0	0	0.000	0.000
.1	6.06	.19	39	.731	2.41
.2	6.04	.46	46	.878	3.12
.3	6.00	.76	39	.754	3.04
.4	5.98	1.00	49	.954	3.88
.5	5.93	1.26	44	.872	4.00
.6	5.82	1.70	27	.556	3.72
.7	5.76	1.92	32	.674	3.93

Pressure-200 psig

0	6.07	0	0	0.000	0.000
.1	6.05	.26	17	.323	1.24
.2	6.01	.51	35	.675	2.55
.3	6.00	.77	52	1.007	3.81
.4	5.97	1.04	65	1.270	4.87
.5	5.90	1.40	71	1.423	5.63
.6	5.76	1.88	42	.884	4.52
.7	5.70	2.09	45	.969	4.97

Pressure-300 psig

0	6.07	0	0	0.000	0.000
.1	6.01	.51	27	.520	2.08
.2	5.97	1.04	36	.703	3.16
.3	5.82	1.70	13	.268	2.50
.4	5.62	2.26			
.5	5.50	2.57			
.6	5.27	2.96			
.7	4.90	3.63			

TABLE III

Function Values - Case I

	t = .1 sec.	t = .2 sec.	t = .3 sec.	t = .4 sec.	t = .5 sec.	t = .6 sec	t = .7 sec.
				Pressure = 100 psig			
(x-c)	y	y	y	y	y	y	y
0	2.41	3.12	3.04	3.88	4.00	3.72	3.93
1	1.347	1.846	1.95	2.498	2.623	2.558	2.955
2	.932	1.349	1.514	1.954	2.128	2.244	2.572
3	.669	1.033	1.247	1.614	1.813	2.043	2.329
4	.477	.800	1.048	1.361	1.586	1.896	2.152
5	.324	.617	.891	1.162	1.401	1.780	2.011
a	0.19	0.46	0.76	1.00	1.26	1.70	1.920
				Pressure = 200 psig			
0	1.240	2.55	3.81	4.87	5.63	4.52	4.97
1	.772	1.574	2.353	3.037	3.617	3.236	3.569
2	.587	1.190	1.782	2.307	2.808	2.734	3.018
3	.471	.947	1.421	1.860	2.298	2.417	2.668
4	.386	.769	1.154	1.525	1.921	2.183	2.413
5	.318	.627	.944	1.260	1.623	1.999	2.210
a	.26	.51	.77	1.04	1.40	1.88	2.09
				Pressure = 300 psig			
0	2.08	3.16	2.50				
1	1.850	2.143	2.114				
2	1.033	1.743	1.962				
3	.846	1.491	1.865				
4	.709	1.305	1.795				
5	.600	1.158	1.739				
a	.51	1.04	1.70				

Values of a, h, v, and F are given in Table II. The value, h, is presented as positive since the X-axis of Fig. 10 is arbitrarily set positive downward. In computing F, r is taken as equal to $(\pi A)^{\frac{1}{2}} (\pi+2)^{-\frac{1}{2}}$ where A is the outlet area and where r is the effective radius of the discharge jet at conditions of assumption 1, namely, uniform and parallel flow. This value is approximately .308 inches.

Values of y with respect to x-c are given in Table III for various indicated charging pressures and times after discharge. Isochrons are presented in Figs. 11-12 from values in Table II. These describe the two-dimensional profile of the interface pattern in accordance with the mathematical model of Case I.

2. Case II

This case deals with the theoretical formation of a circular cylindrical vortex, exposed to a uniform surface pressure and subjected to a uniform downward acceleration. By equating the vortex cavity to Table values of V_1, the vortex surface for instantaneous values of acceleration and surface pressure may be approximated. It should be noted that uniform downward acceleration of the proposed vortex surface can occur only if the liquid is inviscid.

Case II must, therefore, be based on two assumptions:

(1) The interface behaves as a surface of constant pressure based on Rankine's combined vortex.

(2) The fluid is inviscid.

Utilizing these assumptions the following relationship exists: Letting y = ordinate of a surface point with respect to the initial liquid level.

x = abscissa of the point with respect to the vortex center.

r = effective outlet radius

b = vortex boundary radius

a = interface radius

h = ordinate of interface - container demarcation with respect to the initial level. (This also is taken as the general liquid level)

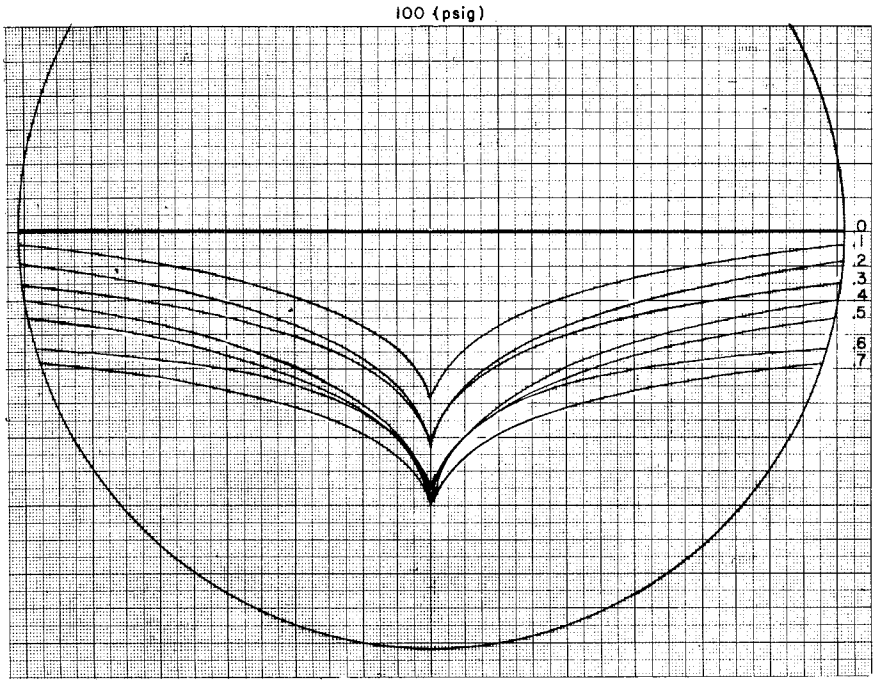

Fig 11a Isochron Interface Profiles With Initial Pressure of 100 psig (per Case I)

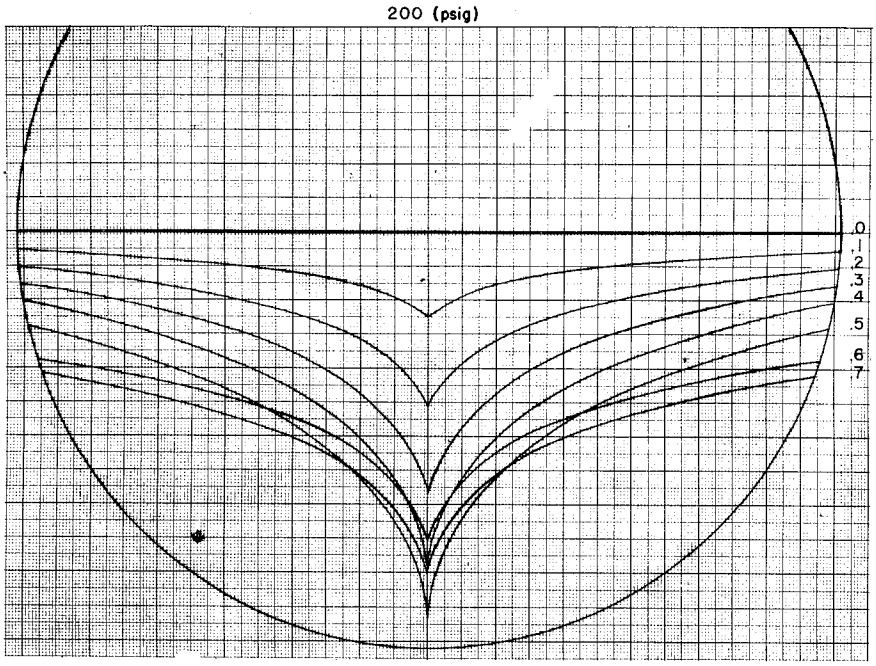

Fig 12a Isochron Interface Profiles With Initial Pressure of 200 psig (per Case I)

F = instantaneous acceleration

$\frac{\omega}{2}$ = anguler velocity of vortex

V_1 = interface distortion volume

The surface equations for the vortex profile become;

(1) $y = \frac{b^4 \omega^2}{2Fx^2}$, when $x > b$

(2) $y = \frac{b^2 \omega^2}{F}\left(1 - \frac{x^2}{2b^2}\right)$, when $x \leq b$

Assuming a positive direction as down for x values the value V_1 as a function of the volume of rotation of (1) and (2) about the X-axis becomes:

$$\frac{V_1}{2\pi} = \int_0^b \int_0^{\frac{b^2\omega^2}{F}\left(1-\frac{x^2}{2b^2}\right)} x \, dy dx + \int_b^a \int_0^{\frac{b^4\omega^2}{2Fx^2}} x \, dy dx$$

Solving:

(3) $$\frac{4V_1F}{\pi} = \omega^2 b^4 \left(3 + 4\ln\frac{a}{b}\right)$$

but:

(4) $$\omega^2 = \frac{2Fa^2h}{b^4}$$ when $y=h$ and $x=a$ are substituted in equation (1), (3) and (4) then yield

(5) $$\ln b = \ln a + .75 - \frac{V_1}{2\pi a^2 h}$$

Equation (1) may now be solved for $\frac{\omega^2}{F}$ using computed values of b from equation (5) and values of a and h from the data. The value $\frac{\omega^2}{F}$ also holds for equation (2).

The two-dimensional profile of the vortex surface may therefore be computed.

A few calculations indicate that the above model profile quickly degenerates into a parabola since the boundary radius approaches and exceeds the value, a, as time after discharge progresses. A purely parabolic profile is inconsistent with observed details of the interface pattern. Obviously Case II can only apply if the Rankine combined vortex gives way to the more general form of a hollow circular vortex. Insufficient data is presented in this report to explore this more general form.

C. CONCLUSIONS

Precision measurement of physical phenomena effectively differentiates between plausible and actual situations. Computations based on measurements of the interface container demarcation and the container pressure indicate distortion of the interface. Actually a complex contour develops in the surface. The contour is sufficiently divergent from planer that bypass of the propellant occurs. Indeed, although surface detail was poorly resolved on the high-speed film record, sufficient detail was obtained to indicate a definite bypass activity. The activity seemed to occur when the demarcation line had receded from three to four inches below initial conditions. However, resolution of the surface was so poor that precise measurements of flow details could not be obtained. Thus only plausible conditions can be inferred.

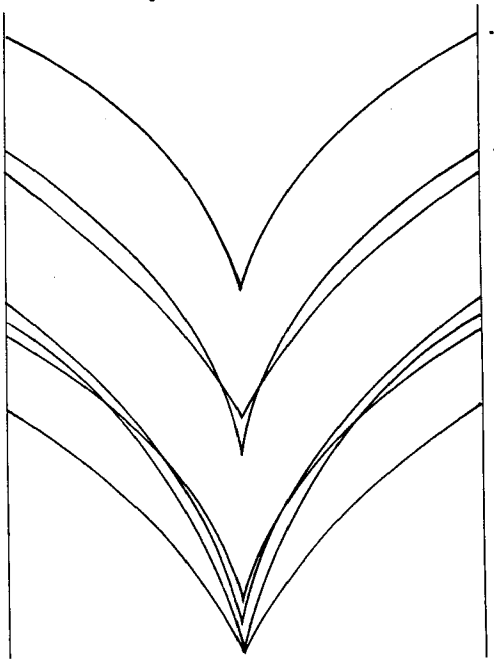

Fig 11b Case I - Isochron Profile Close-up at 100 psig

Two conditions are considered, namely, Cases I and II. Case II degenerates into a general vortex pattern which cannot be exploited since details of vortex strength and boundary conditions are lacking. Case I considers the surface as a thin circular elastomeric membrane restrained at the edge and centrally loaded. Though not an exact picture of the interface profile Case I presents information from which certain inferences may be drawn. As one observes Figures 11 and 12 it may readily be seen that the isochrons tend to cluster near the center with a certain periodicity. This can be indicative of but one general process. As the

central portion of the surface becomes depressed a kinetic head is built up at the edge. Eventually, this head offsets the dampening effect of the fluid viscosity and returns the surface to more stable conditions. As the main flow is from the center of the surface, however, the edge never quite catches up and eventually bypass occurs as the interface center dips through the outlet. This tendency also increases with increasing values of the ratio of the interface radius to the effective outlet radius. No evidence was noted which would indicate the necessity for streamlining the fixtures normally found in the B1A containers.

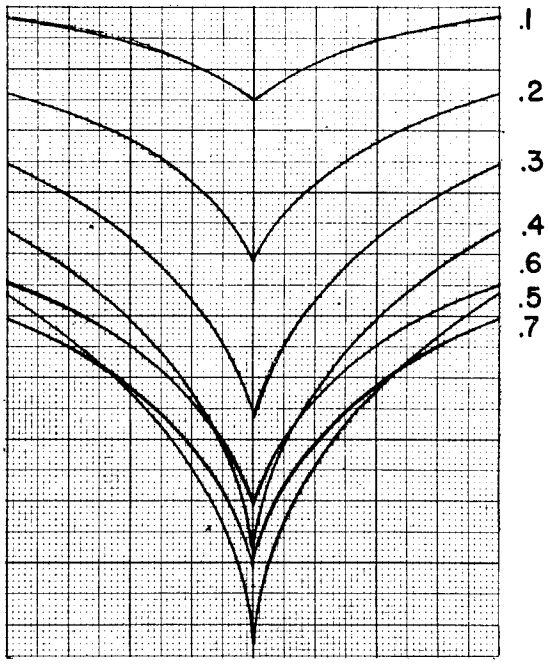

Fig 12b Case I - Isochron Profile Close-up at 200 psig

The above case is inconclusive in that a direct relation has not been established for considering fluids of viscosities and densities other than triethylene glycol.

D. RECOMMENDED FUTURE EFFORTS

With the use of high rate discharge systems the limitations imposed on airborne extinguishing systems by the gas-liquid interface distortion in the storage container become increasingly important. Obviously some limiting value exists for the ratio of the radius of the initial interface to that of the outlet. Beyond this value, inefficiencies arise as a result of propellent bypass. Increased agent mass requirements might then require a container designed in the form of a cylinder, for example, rather than a sphere. An effort should therefore be made to establish the interface distortion as a function of the ratio of the radii of the sphere and of the outlet port, the agent used and the initial pressure.

Surface detail for the extinguishing agents used in this study was immeasurable. An attempt should be made to photograph the interface of the various extinguishing agents to relate the interface pattern to that of the triethylene-glycol used in this study. This might be done through prudent choice of antifoaming agents and/or by adjustment of the light reflecting properties of the container walls with suitable coating material. Details of flow in the interface

might be obtained through the incorporation of foreign material such as small quantities of metal powder.

A study might be made to determine the effect of various container surface contours in the region of the outlet port. One might speculate on the possible efficiencies of unique container shapes including that of the surface of revolution of a four-cusp hypocycloid. Replacing a sphere with such a configuration would, however, increase the radius of space needed by about 60% in order to maintain the same volume.

BIBLIOGRAPHY

1. Lamb, Horace, Hydrodynamics, 6th Edition, Dover Publications, New York, 1945

2. Wilne-Thomson, L. M., Theoretical Hydrodynamics, Third Edition, MacMillan Co., New York, 1957.

3. Russell, George E., Hydraulics, Fifth Edition, Henry Holt & Co., New York, 1942.

4. Pauw, Adrian, Sangster, William M. and Crabtree, Robert G., Light-Weight Fire Extinguishing System Container, WADC Technical Report 55-338. Wright Air Development Center, Wright-Patterson Air Force Base, Ohio, December 1955.

5. Wood, Horace W., Sangster, William M. and Petersen, Jack S., Study of Fire Extinguisher Flow Rate, AF Technical Report 6430. Wright Air Development Center, Wright-Patterson Air Force Base, Ohio, December 1953.

APPENDIX A

MATHEMATICAL TREATMENT OF FILM RECORD

Consider Figure I3

Let O be the center of the container

Let the initial gas-liquid interface lie on the X-axis.

Let C be the nodal point of the photographic optic system

Let I be the center of the outlet port

Let the circle be the intersection of the plane defined by the points O, C and I and the internal surface of the container.

From direct measurement the location of C in inches is (-8.81, 8.8)

The slope of the film plane with respect to the X-axis is $40^{\circ}30'$.

The radius of the circle is 6.07 inches.

1. The equation of the circle is $x^2 + y^2 = 36.8$

   Construct the line AB tangent to the circle at T and with a slope of $40^{\circ}30'$.

   The equation of AB is then $y = x \tan 40^{\circ}30' - \frac{6.07}{\cos 40^{\circ}30'}$

2. or $y = .85x - 7.99$

   Construct the line CF through I

   The equation of CF is then $y = -x \frac{8.8 + 6.07}{8.81} - 6.07$

3. or $y = -1.69x - 6.07$

   Construct the line CG through H

   The equation of CG is then $y = \frac{8.8}{-8.81-6.07} (x-6.07)$

4. or $y = -.59x + 3.59$

   solving 2 and 3 gives the location of point F

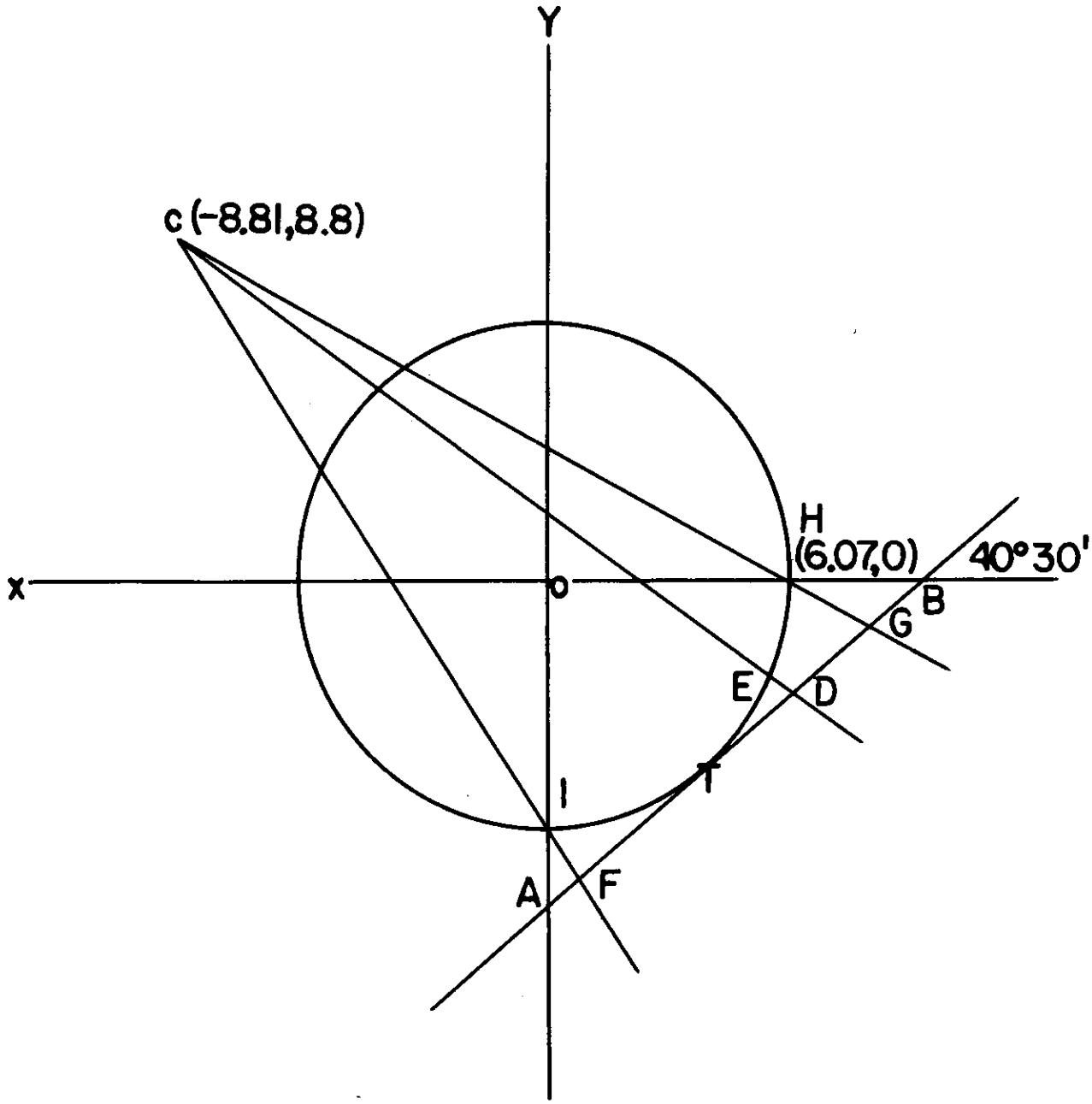

Fig 13 Film Image Interpretation

TABULATION OF REDUCED DATA

Test Nr/9 TEG at 100 psig

Observation	Time (sec)	DG/FG	Equation of CED	Simultaneous equation of CED and circle	Coordinates of E	
					x	y
1	.147	.031	$y=-.61x+3.42$	$1.37x^2-4.17x-25.10=0$	6.06	-.28
2	.260	.072	$y=-.64x+3.19$	$1.41x^2-4.08x-26.62=0$	6.02	-.66
3	.381	.105	$y=-.66x+2.99$	$1.44x^2-3.95x-27.86=0$	5.98	-.96
4	.499	.138	$y=-.68x+2.79$	$1.46x^2-3.79x-29.02=0$	5.94	-1.25
5	.617	.198	$y=-.72x+2.40$	$1.52x^2-3.45x-31.05=0$	5.80	-1.78
6	.780	.228	$y=-.75x+2.21$	$1.56x^2-3.31x-31.92=0$	5.71	-2.07
7	.813	.252	$y=-.77x+2.04$	$1.59x^2-3.14x-32.64=0$	5.62	-2.29
8	.984	.279	$y=-.79x+1.86$	$1.62x^2-2.94x-33.34=0$	5.53	-2.51
9	1.111	.333	$y=-.83x+1.45$	$1.69x^2-2.41x-34.70=0$	5.34	-2.98
10	1.175	.362	$y=-.85x+1.17$	$1.72x^2-1.99x-35.43=0$	5.15	-3.21
11	1.303	.398	$y=-.89x+.95$	$1.79x^2-1.69x-35.90=0$	4.97	-3.48
12	1.377	.455	$y=-.94x+.49$	$1.88x^2-.92x-36.56=0$	4.66	-3.89
13	1.485	.486	$y=-.97x+.22$	$1.94x^2-.43x-36.75=0$	4.46	-4.11
14	1.586	.554	$y=1.04x-.40$	$2.08x^2+.83x-36.64=0$	4.00	-4.56

*Volume of remaining liquid if interface is not distorted (cu. in.)

436	110
391	80
357	65
325	40
268	
238	
216	
195	
153	
132	

*Vo= 469 cu. in.

Test Nr/10 — TEG at 200 psig

Observation	Time (sec)	DG/FG	Equation of CED	Simultaneous equation of CED and Circle	Coordinates of E x	Coordinates of E y	*Volume of remaining liquid if interface is not distorted (cu.in.)
1	.375	.109	$y=-.66x+2.97$	$1.44x^2-3.92x-27.99=0$	5.97	-.97	355
2	.492	.152	$y=-.69x+2.70$	$1.48x^2-3.73x-29.51=0$	5.90	-1.37	312
3	.611	.216	$y=-.74x+2.29$	$1.55x^2-3.39x-31.56=0$	5.73	-1.95	249
4	.723	.235	$y=-.75x+2.16$	$1.56x^2-3.24x-32.14=0$	5.71	-2.12	235
5	.836	.277	$y=-.79x+1.87$	$1.62x^2-2.95x-33.30=0$	5.54	-2.51	195
6	.945	.327	$y=-.83x+1.50$	$1.69x^2-2.49x-34.55=0$	5.32	-2.92	156
7	1.053	.379	$y=-.87x+1.11$	$1.76x^2-1.93x-35.57=0$	5.08	-3.31	123
8	1.131	.424	$y=-.91x+.74$	$1.83x^2-1.35x-36.55=0$	4.85	-3.68	96
9	1.263	.522	$y=-1.01x-.11$	$2.02x^2+.22x-36.79=0$	4.22	-4.48	47
10	1.364	.578	$y=-1.07x-.63$	$2.14x^2+1.30x-36.40=0$	3.83	-4.73	32
11	1.465	.642	$y=-1.14x-1.29$	$2.30x^2+2.94x-35.14=0$	3.32	-5.07	18
12	1.565	.692	$y=-1.20x-1.83$	$2.44x^2+4.39x-33.45=0$	2.91	-5.32	4
13	1.664	.725	$y=-1.25x-2.20$	$2.56x^2+5.50x-31.96=0$	2.64	-5.50	2
14	1.761	Empty					

*V_o=469 cu. in.

Test Nr/14

Observation	Time (sec)	DG/FG	Equation of CED	Simultaneous equation of CED and Circle	Coordinates of E x	Coordinates of E y	*Volume of remaining liquid if interface is not distorted (cu.in.)
1	.271	.166	$y=-.70x+2.62$	$1.49x^2-3.67x-29.94=0$	5.88	-1.50	316
2	.378	244	$y=-.76x+2.10$	$1.58x^2-3.19x-32.39=0$	5.65	-2.19	225
3	.514	.288	$y=-.80x+1.78$	$1.64x^2-2.85x-33.64=0$	5.48	-2.61	185
4	.609	.339	$y=-.84x+1.41$	$1.71x^2-2.37x-34.81=0$	5.25	-3.00	149
5	.714	.429	$y=-.92x+.71$	$1.85x^2-1.31x-36.30=0$	4.84	-3.74	92
6	.760	.482	$y=-.97x+.24$	$1.94x^2-.47x-36.75=0$	4.47	-4.10	66
7	.833	.535	$y=-1.03x-.22$	$2.06x^2+.45x-36.75=0$	4.14	-4.48	45
8	.914	.588	$y=-1.08x-.73$	$2.17x^2+1.58x-36.27=0$	3.74	-4.77	30
9	1.048	Empty					

*Vo = 469 cu. in.

5. as (.76, -7.35)

solving 2 and 4 gives the location of point G as

6. (8.04, -1.15)

A point D is located on line AB with coordinates $(x_1, y1)$. The point is so located that the distances DG and FD are proportional to the apparent film image distances of the initial interface-container demarcation and outlet center to the interface-container demarcation for any specific time, t, during discharge. The line CD is then drawn intersecting the circle at E.

The equation of line CD becomes

7. $$y - y_1 = \frac{(x-x_1)(y_1-8.8)}{(x_1+8.81)}$$

Solution of equations 1 and 7 then gives the true position of the interface-container demarcation for time, t.

It should be noted that the intersection of the plane CAB and the film plane falls at an angle of 88° to the horizontal of the film plane image. The ratio DG/FD is therefore found from film image measurements along this intersection.

The accompanying tabulation of reduced data contains the ratio DG/FG versus time after discharge as computed from the photographic record. Equations for the line CED are then given for each recorded time. The simultaneous equation for the circle and line CED is given for each time. The solution of each simultaneous equation for E is recorded. PtE then represents the true demarcation position between interface and container wall for the indicated time.

The formula $V = 1/6\ \pi (6.07 + y) \left[(6.07 + y)^2 + 3x^2\right]$ where x and y are the coordinants of E, and V is the volume of liquid remaining in the sphere, denotes the residue of liquid for a particular time after discharge if no interface distortion occurs. Values of V for the various times are recorded in the tabulation.

APPENDIX B

PRESSURE DATA

The following pressure data with respect to time were obtained during actual discharge tests. The data were collected by means of a strain gage pressure transducer connected to an oscillograph. Remaining liquid volume V_p as a function of time is also recorded. V_p was calculated from the relationship, $V_p = 938 - (p_o V_o^{\gamma}/p_1)^{1/\gamma}$ where p_o = initial pressure, V_o = initial volume, p_1 = pressure volume from data for any time, t, after discharge and γ = ratio of specific heats for N_2 = approximately 1.40. The relationship holds true only until propellant bypass occurs.

Test Nr. 9			Test Nr. 10			Test Nr. 14		
Time (sec.)	Pressure (psia)	Vp (cu. in.)	Time (sec.)	Pressure (psia)	Vp (cu. in.)	Time (sec.)	Pressure (psia)	Vp (cu. in.)
0.000	114.4	469	0.000	214.4	469	0.000	314.4	469
0.147	92.4	392	0.375	137.4	293	0.271	201.9	294
0.260	83.4	351	0.492	122.8	239	0.378	182.1	245
0.381	75.4	307	0.611	116.4	212	0.514	158.9	174
0.499	71.4	282	0.723	110.6	185	0.609	150.0	142
0.617	66.4	247	0.836	103.2	147	0.714	139.4	99
0.780	60.4	198	0.945	97.5	114	0.760	135.8	84
0.813	58.4	180	1.053	91.8	78	0.833	129.4	53
0.984	56.4	161	1.131	89.9	65	0.914	124.0	26
1.111	56.4	161	1.263	84.3	24	1.048	110.9	
1.175	54.4	141	1.364	80.5				
1.303	49.4	82	1.465	76.3				
1.377	48.4	72	1.565	69.2				
1.485	46.4	45	1.664	63.5				
1.586	45.4	31	1.761	55.9				

APPENDIX C

PHYSICAL PROPERTIES OF LIQUID PHASES

	BT	DB	CB	Carbon Dioxide	Triethylene-glycol
Chemical formula	$CBrF_3$	CBr_2F_2	CH_2BrCl	CO_2	$C_6H_{12}(OH)_2$
Molecular weight	148.9	209.8	129.4	44.	150.2
Boiling Point (°F)	-72.0	76.1	152.6	-109.3	549.5
Freezing point (°F)	-270.4	-222.9	-123.7	-109.3	19.0
Critical Temp (°F)	152.6	388.7	531.0	87.8	-
Critical Press (psia)	575.0	600.0	--	1075.	-
Critical Density (Lbs/ft^3)	46.5	52.7	40.0	-	-
Density at 70°F (Lbs/ft^3)	98.0	142.3	120.5	-	70.1
Vapor pressure at 70°F (psia)	225.	13.	2.8	830.	< .002
Viscosity 70°F (centipoises)	0.23	0.33	0.64	-	45.